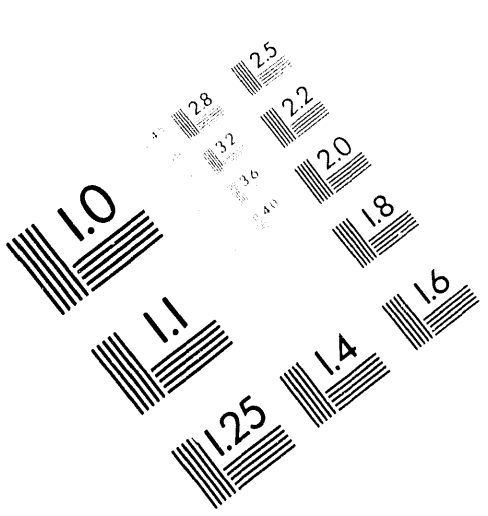

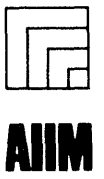

AIIM

Association for Information and Image Management

1100 Wayne Avenue, Suite 1100
Silver Spring, Maryland 20910

301 587-8202

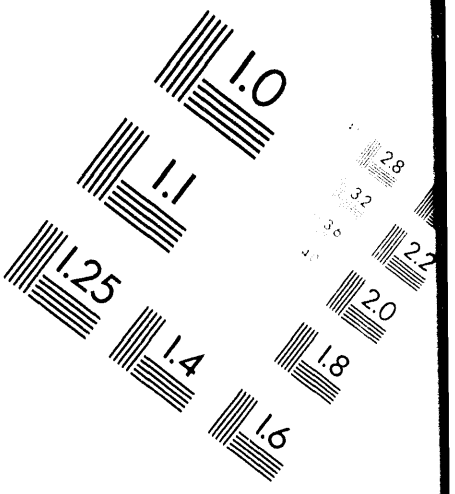

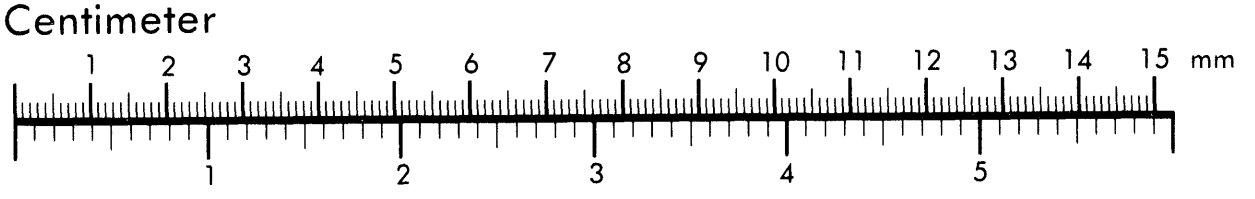

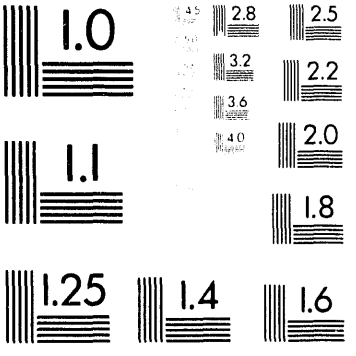

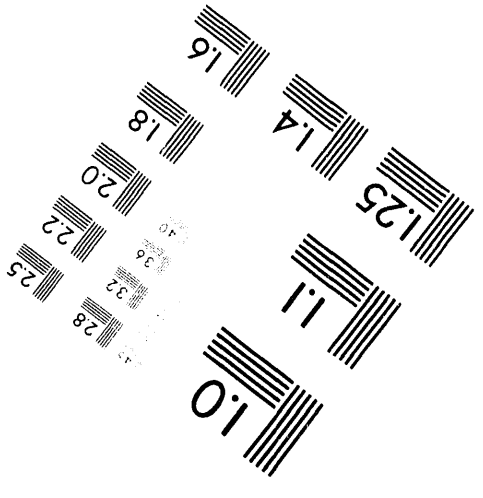

MANUFACTURED TO AIIM STANDARDS
BY APPLIED IMAGE, INC.

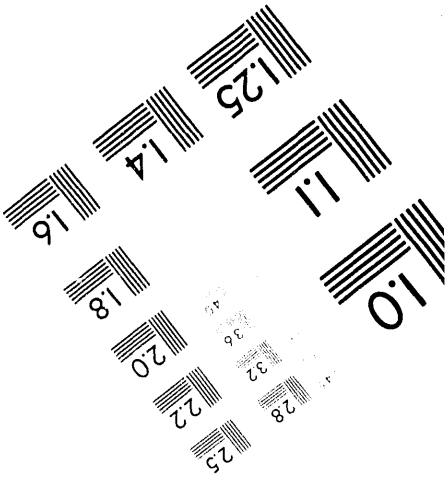

1 of 1

PNL-9469
UC-713
UC-506

LABORATORY SENSOR DESIGN FOR FIBER-OPTIC DETECTION OF ^{85}Kr (U)

B. D. Geelhood
M. A. Knopf

June 1994

Prepared for
the U.S. Department of Energy
under Contract DE-AC06-76RLO 1830

Pacific Northwest Laboratory
Richland, Washington 99352

EXECUTIVE SUMMARY

The goal of the fiber-optic detection of ^{85}Kr project is to produce a sensor to detect ^{85}Kr in real-time from either an airborne or ground-based platform. The ^{85}Kr gas is a fission product which is released in large quantities during fuel reprocessing and in minor quantities during nuclear reactor operations. Thus an airborne plume of ^{85}Kr is a radioactive signature of proliferation. Since ^{85}Kr has a 10.72 year half life, it is difficult for a proliferator to contain the gas for several half lives to avoid releasing the radioactive signature of proliferation. The long half life also results in a plume that can extend several kilometers from the source, which allows initial proliferation monitoring from large distances. The sensor can be used to make stand-alone, real-time measurements of ^{85}Kr that can be used as direct evidence for proliferation and/or as a screening sensor to determine when to collect air samples for further laboratory analysis.

This report provides a summary of the ^{85}Kr beta sensor design that PNL will use in the laboratory to: 1) demonstrate the measurement technique, 2) establish minimum detection limits, and 3) optimize the sensor design for the final airborne sensor package. The goal of the final airborne sensor package will be to measure ^{85}Kr at activity levels as low as or as close to ambient background levels as possible with a reasonably sized sensor.

This report outlines the technique that will be used to measure ^{85}Kr, the modular sensor design, the design details of the multilayer modules, the proposed signals to be recorded from the laboratory sensor, the electronics required to produce the signals, and proposed laboratory measurements to demonstrate and optimize the sensor capabilities.

CONTENTS

INTRODUCTION

The fiber-optic detection of ^{85}Kr project being conducted by Pacific Northwest Laboratory[a] will produce a sensor to detect ^{85}Kr by keying on the relatively low-energy beta particle emitted during ^{85}Kr decay. Figure 1 shows the ^{85}Kr decay scheme.

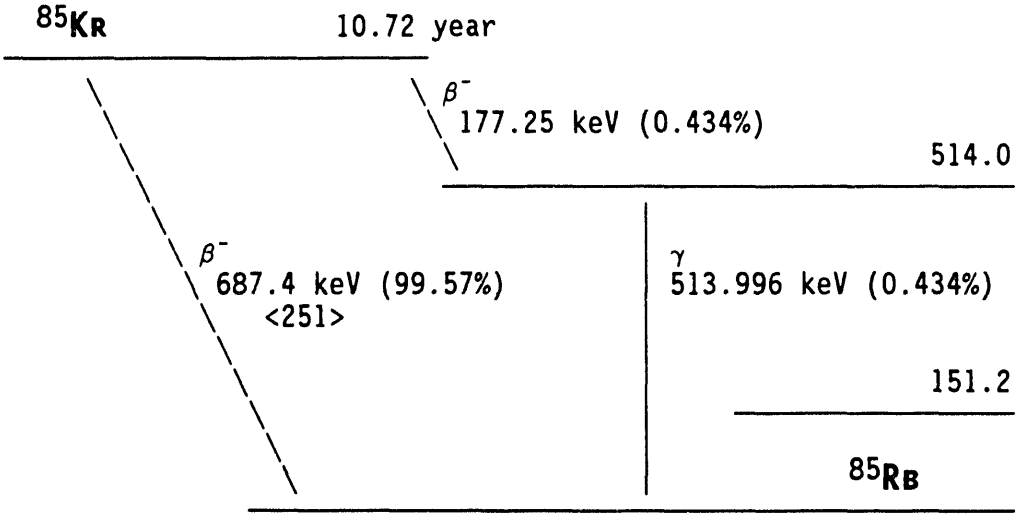

FIGURE 1. ^{85}Kr Decay Scheme

The 687-keV maximum-energy beta decay provides the best means of detecting this isotope. The 514-keV gamma ray has a low intensity (or path fraction) and is very close to both the 511.0-keV annihilation gamma ray and the ^{208}Tl 510.6-keV (21.6%) gamma ray, which are both commonly found in background spectra.

The beta particle has a reasonable range in air and will interact with fiber optic scintillators. The basic detection scheme uses several layers or mats of plastic scintillating fibers. Detection in a layer requires detection

[a] Pacific Northwest Laboratory is operated for the U.S. Department of Energy by Battelle Memorial Institute under contract DE-AC06-76RLO 1830.

of an optical photon (scintillation light) in the photomultiplier at each end of the fiber layer within a 20-ns time window.

Energetic beta particles incident on the multilayer sensor penetrate through several fiber optic layers, interacting with and being detected in each layer they pass through. The detection signature for energetic beta particles is the production of coincidence detections in several consecutive layers starting with the first layer. Since less-energetic beta particles incident on the sensor penetrate fewer layers, the detection signature for low-energy beta particles is the production of a coincidence detection in only the first layer. In a crude fashion the number of consecutive layers with a coincidence detection indicates the incident beta particle energy.

Unlike beta particles, gamma rays do not interact with every layer they pass through. Thus gamma rays may produce coincidence detections in only the internal layers without a coincidence detection in the front layer. Cosmic-ray charged particles tend to interact with all the layers. The sensor will use the various combinations of multilayer coincidence detections to selectively detect the ^{85}Kr beta.

During beta decay, both a beta particle (electron) and a neutrino are emitted with the decay energy shared between them. Thus the energy distribution of the beta particle ranges from zero to a maximum value (687 keV in the case of ^{85}Kr).

SENSOR DESIGN

The fiber-optic detection of ^{85}Kr airborne sensor will have fiber-optic sensor modules placed on the inner wall of a large-diameter (0.5 to 1.0 meter diameter) cylinder containing the rapidly flowing, real-time air sample. The fibers will be aligned parallel to the cylinder axis with photomultiplier tubes (PMTs) at each end. The plastic scintillator fibers will be 1.25 meters long with a 1-meter flat section centered in each module. The remaining length at each end allows bundling the fibers to the PMTs. The 1/e light attenuation distance of the BF-10 Bicron plastic scintillator fibers is about 1.6 meters. Since detectable scintillation light output from the 0.5-mm front layer is at a premium, it is not efficient to use longer fiber lengths. Also, the 1.5-meter sensor length (with PMTs) should be able to fit in a standard aircraft pod. An option for the airborne sensor will be to have additional fiber mats on the horizontal diameter to improve spatial uniformity and detection efficiency.

The laboratory sensor design will include two different sensor module concepts, one with beta particles incident from only one side of the mats (wall modules) and the other with beta particles incident from both sides (diameter modules). Figure 2 shows the module design with beta particles incident from only one side. This design uses five layers of optical fibers and would be used at the cylinder wall. The thin, black plastic front face blocks alpha particles and makes the sensor module light tight. It is also washable and/or replaceable to reduce buildup of radioisotopes in the sensor. The passive slab of polyethylene blocks energetic source betas from the cosmic-ray anticoincidence layer (#5). This layer should be low-Z to minimize gamma-ray interaction probabilities.

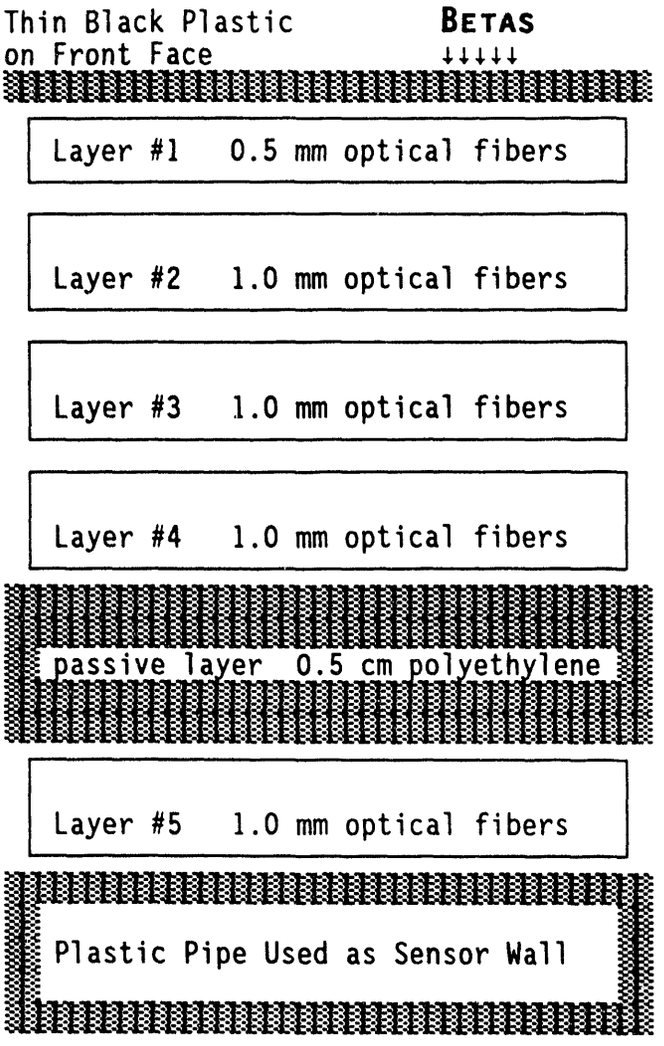

	- Net Coincidence Counts - ^{36}Cl	Background
Layer #1 0.5 mm optical fibers	2100 cps [469 cps	8 cps 14 cps]*
Layer #2 1.0 mm optical fibers	1200 cps	18 cps
Layer #3 1.0 mm optical fibers	73 cps	18 cps
Layer #4 1.0 mm optical fibers	7 cps	18 cps
Layer #5 1.0 mm optical fibers	5 cps	17 cps

* ==> old 1 μs electronics

FIGURE 2. Initial Prototype Sensor Design

On the right side of the figure, net coincidence count rates are listed that show how the sensor is expected to operate. The beta from ^{36}Cl has an average energy of 245 keV, which is nearly the same as the 251-keV average energy ^{85}Kr beta. Thus the ^{36}Cl was used as an experimental analog for the ^{85}Kr beta in the initial tests to determine sensor design. The observed net coincidence count rates show that the ^{36}Cl beta <245 keV> produces sufficient counts in the first two layers of this sensor to allow high detection efficiency for the ^{85}Kr beta. The background rate is largely due to cosmic-

ray particles that interact with all the layers. The ^{36}Cl beta source produced a few net counts in the third and subsequent layers due to either betas near the peak of the beta-energy distribution or Bremsstrahlung gamma rays. Bremsstrahlung gamma rays, which are produced by deceleration of the beta particle, are more penetrating than beta particles of the same energy.

The thickness and number of layers in this design allow for rejecting (on an event-by-event basis) more energetic beta particles that will produce coincident detections in more than 2 layers. The thinner front layer also allows detection of beta particles less energetic than ^{85}Kr by a change in the ratio of detections in only the first layer to detections in both the first and second layer. The thinner front layer also reduces the probability of gamma-ray detection in the first layer by providing less mass for gamma-ray interaction. Many gamma rays can be rejected (on an event-by-event basis) due to interaction in only internal layers, but those detected in the first layer will have to be removed statistically by subtracting an estimated contribution to the ^{85}Kr count rate based on the count rate in internal layers only. Most cosmic-ray particles can be rejected (on an event-by-event basis) due to interaction in all the layers.

The electronics utilize a 20-ns coincidence window and unstretched PMT pulses rather than the previous electronics with a 1-μs coincidence window and stretched PMT pulses. The new electronics greatly improve expected sensor performance. The background coincidence rates are lower than the nominal 14 cps obtained with previous 1-μs electronics due to the lower chance coincidence rates possible with the fast electronics. Also, the detection efficiency for the ^{36}Cl beta is considerably higher because the new electronics have much better noise characteristics that allow the discriminator threshold to be well below the 1-PE[a] peak. This improves the coincidence efficiency (1-PE at each fiber end) as the square of the efficiency for detecting 1-PE signals at one end. The fast electronics allow a significant reduction in the minimum detectable activity for the sensor.

(a) A 1-PE single refers to one detected optical photon, which ejects one photoelectron from the photocathode of the PMT. This one photoelectron is multiplied to about a million electrons as it cascades down the PMT dynode chain as each incidenct electron knocks about five secondary electrons off each dynode.

The ^{36}Cl source had an activity of 2.152E6 dpm (6-3-92) or 3.518E4 β/s with a 98.1% beta path. The 2100-cps first-layer coincidence rate corresponds to at least an efficiency of 12% for the half of the betas headed in the sensor direction. Since the source was only about 2 cm from the ribbon, assuming a hemisphere of solid angle is both reasonable and conservative.

Note that for betas directly incident on 1-mm fibers, the ^{36}Cl coincidence rate is 3500 cps (up from 407 cps with the old electronics) and the background rate is 18 cps (down from 21-40 cps). Also for betas directly incident on 0.25-mm fibers, the ^{36}Cl coincidence rate is 600 cps and the background rate is 2 cps. Thus, using the 0.5-mm fiber on the front face does not greatly reduce ^{36}Cl detection efficiency, but using 0.25-mm fibers unacceptably lowers ^{36}Cl detection efficiency. The effective detection efficiency using 0.5-mm fibers for coincidence detections between the first two layers can be increased back near the 1-mm efficiency by requiring a 1-PE detection at only one end of the 0.5-mm fiber because dark count is eliminated by the coincidence requirement at both ends of the second layer.

Figure 3 shows the design with beta particles incident from both sides. This design uses six layers of optical fibers and would be used in the plane containing the cylinder axis and the horizontal diameter.

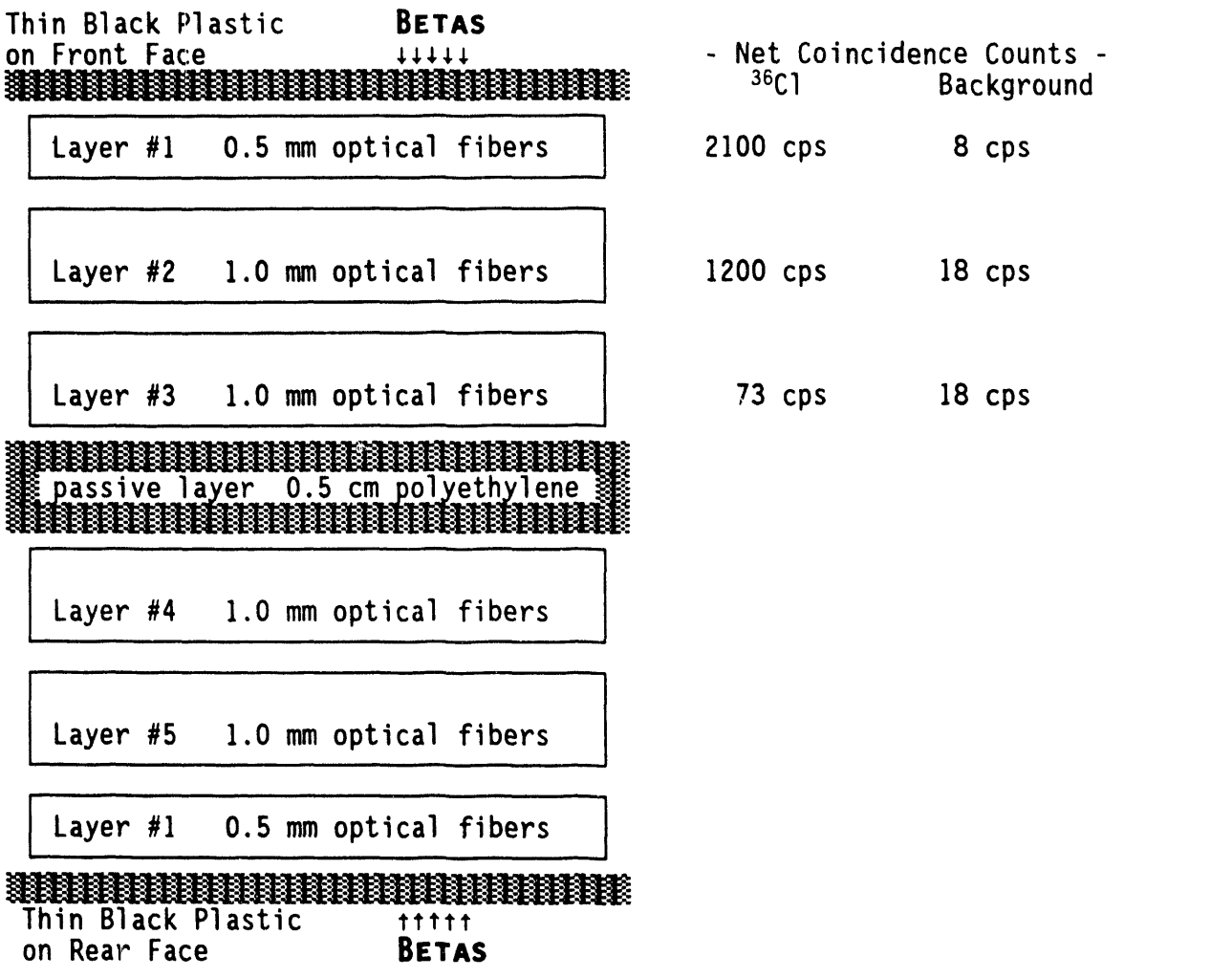

FIGURE 3. Alternate Prototype Sensor Design

DATA RECORDING

The laboratory demonstration sensor system will record the count rates listed in Tables 1 and 2. Note a layer count requires at least a 1-PE detection at each end of the fiber layer (double-ended 20-ns coincidence in the layer). The laboratory demonstration will record more information channels than the deployed airborne sensor to determine experimentally the optimum signals to allow the lowest minimum detectable levels of ^{85}Kr. In the tables, the first column lists the counter number (18 separate counters used). The second column lists the criteria for an event to increment that counter. The last column lists physical causes for events that increment particular counters.

TABLE 1. Data Recording Scheme for 5-Layer Sensor

Counter	Requirements	Cause
#1	Layer #1 (other layers possible)	
#2	Layer #2 (other layers possible)	
#3	Layer #3 (other layers possible)	
#4	Layer #4 (other layers possible)	
#5	Layer #5 (other layers possible)	
#6	Layer #1 only	very-low-energy betas or gammas
#7	Layers #1 & #2 only	low-energy betas or gammas
#8	Layers #1, #2 & #3 only	medium-energy betas or gammas
#9	Layers #1, #2, #3 & #4 only	high-energy betas or gammas
#10	Layers #1 - #5 (all)	cosmic rays or very-energetic gammas
#11	Layers #2 & #3 only	low-energy gammas
#12	Layers #3 & #4 only	low-energy gammas
#13	Layers #2, #3 & #4 only	medium-energy gammas
#14	Layers #1 & #3 only	between the cracks & chance coinc.
#15	Layers #2 & #4 only	between the cracks & chance coinc.
#16	Layers #4 & #5 only	energetic exterior betas or gammas
#17	Layer #5 only	opposite side betas or gammas
#18	L1A & L1B(delayed)	chance coincidence rate

TABLE 2. Data Recording Scheme for 6-Layer Sensor

Counter	Requirements	Cause
#1	Layer #1 (other layers possible)	
#2	Layer #2 (other layers possible)	
#3	Layer #3 (other layers possible)	
#4	Layer #4 (other layers possible)	
#5	Layer #5 (other layers possible)	
#6	Layer #6 (other layers possible)	
#7	Layer #1 only	very low-energy betas or gammas
#8	Layers #1 & #2 only	low-energy betas or gammas
#9	Layers #1, #2 & #3 only	medium-energy betas or gammas
#10	Layer #6 only	very-low-energy betas or gammas
#11	Layers #6 & #5 only	low-energy betas or gammas
#12	Layers #6, #5 & #4 only	medium-energy betas or gammas
#13	Layers #2 & #3 only	low-energy gammas
#14	Layers #5 & #4 only	low-energy gammas
#15	L (#1 & #3) or (#6 & #4)) only	between the cracks & chance coinc
#16	(#1, #2 or #3) and (#6, #5 or #4)	cosmic rays or very-energetic gammas
#17	Layers #1 - #6 (all)	cosmic rays or very-energetic gammas
#18	L1A & L1B(delayed)	chance coincidence rate

ELECTRONICS

The new fast electronics are easily capable of 20-ns coincidence timing. The 20 ns covers both the nominal 10-ns 1-PE pulse width from the PMT and a maximum optical transit time difference of 8 ns (4-ft fibers), but minimizes chance coincidence rates and is the minimum reasonable coincidence time. The 1-PE amplitude ranges between 100-200 mv with 1/2-inch PMTs, and the discriminator can be easily set well below the 1-PE peak (≈20 mV) while still avoiding most of the electronics noise (≈3-5 mV). Developing these electronics has been a major third-quarter FY93 effort.

The PMT has some after-pulsing following the initial coincident photons that range out to 500 ns. These after pulses may be due to: 1) gas ions in the PMT striking the photocathode, 2) flashes of light at the anode, or 3) photons subsequently released from the scintillator due to either a longer-lived fluorescence lifetime component or trapping. As a result, the electronics will determine and count the intralayer coincidence states that exist within a 20-ns window following the initial double-ended coincidence in a layer (first layer in time to fire). The electronics will then be blocked for the subsequent 500 ns to avoid double-counting events. The blocking pulse will be non-retriggerable and occur following every initial double-ended coincidence (occurring in any of the five layers). The duration of the blocking pulse will be adjustable in the laboratory electronics to allow determination of the optimal blocking time. The normal background and signal count rates in an individual module are expected to be well below any upper limit on the count rate due to the blocking time.

The electronic coincidence logic will start after an amplifier, discriminator, and one-shot associated with each PMT as shown in Figure 4. The amplifier is contained on a small (1 cm x 3 cm) printed circuit board located near the PMT base. The fast discriminator and subsequent one-shot, which determines the pulse width of "L1A", is located on a separate small (2 cm x 4 cm) printed circuit board to separate any logic noise from the sensitive analog front end. The remaining logic for each module will utilize programmable logic arrays for low chip count. Note a double-ended coincidence occurs whenever 20-ns wide pulses from the opposite ends overlap for more than the 2-ns emitter coupled logig (ECL) rise time. The clock input loads a double-ended coincidence indication on the rising edge of the clock input line. Since either pulse can occur first, the double-ended coincidence window is 38 ns, but coincident pulses can be separated by no more than 18 ns.

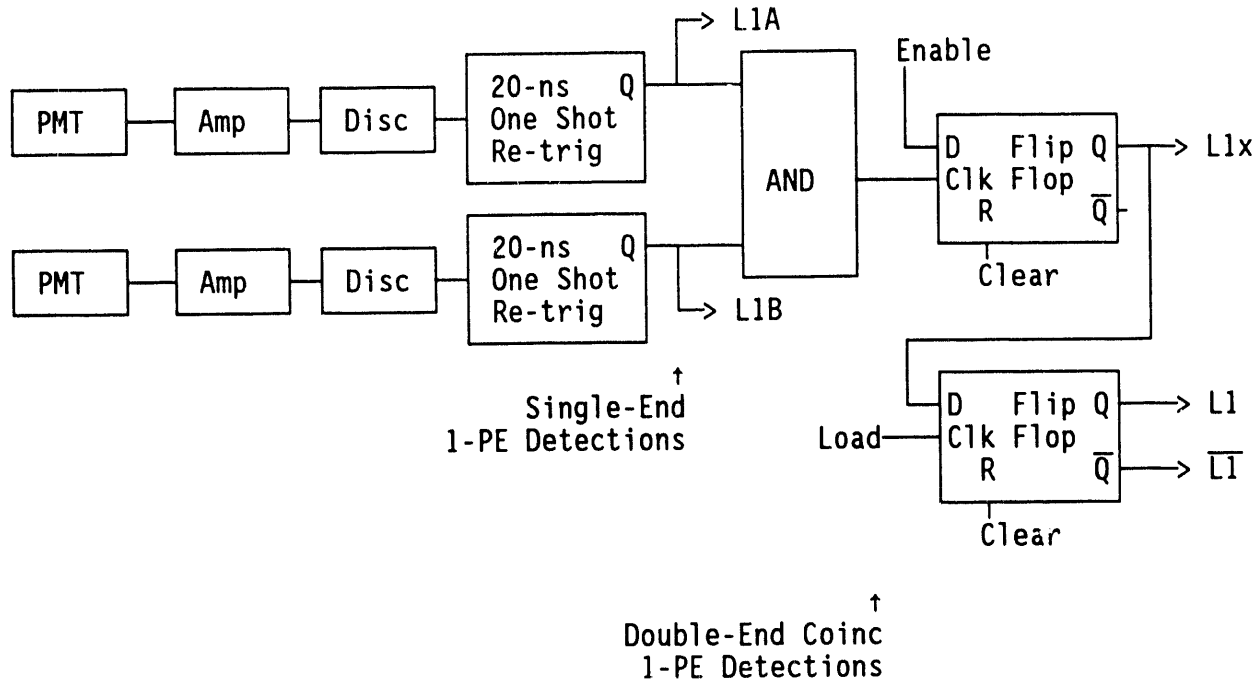

FIGURE 4. Electronic Logic for Each Layer

Figure 5 shows the intralayer coincidence timing logic. The first layer to fire with a double-ended coincidence starts the timing cycle. The signal labeled "L1x" will go high as soon as the AND gate output, which indicates the double-ended coincidence in the layer, clocks the flip-flop. Note "L1x" will stay high until processed. Also, note that the many dark count (non-coincidence) pulses from each PMT are ignored due to the double-ended coincidence requirement. The intralayer coincidences are allowed to settle for 20 ns, which avoids counting a "#1 only", a "#1 & #2 only", and a "#1, #2 & #3 event" if layers #1, #2, and #3 fired sequentially at 3-ns intervals. The beta transit time across all sensor layers is short relative to the 20-ns settling time. At "start + 20 ns" the rising edge of "Load" clocks the "L1x" data into a second flip-flop and "L1" and "$\overline{L1}$" become valid. These are held for 200 ns so the pulse to the counter card is sufficiently wide to produce a count. At "start + 220 ns" the 20-ns wide "Clear" pulse clears all the flip-flop data. The electronics are blocked for 500 ns while the "Enable" line is low to 1) block PMT after-pulses (avoid all double counting) and 2) ensure that every counter pulse returns to the normal state before the next possible count. Note that after "Clear" positively clears a layer's flip-flops, thelow

state of the "Enable" line keeps them clear until the end of the blocking time. It will be necessary to do a "Clear" at power up.

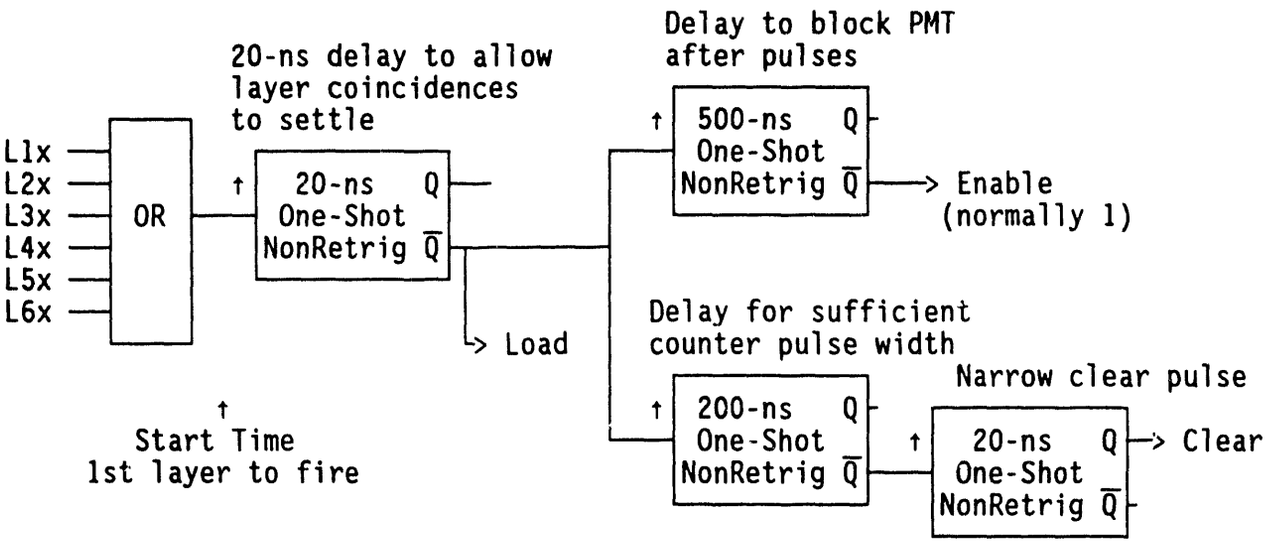

FIGURE 5. Logic for Intralayer Coincidence Timing

Figure 6 shows the proposed coincidence logic, which can be easily implemented in a programmed logic chip. Slight differences in propagation delay (≈2 ns) between the various layer signals (L1 to L6) will not produce sufficiently wide counter pulses to cause false counting.

The L1A and L1B (delayed) mode is intended to provide an experimental chance coincidence rate to allow a possible chance coincidence correction to the ^{85}Kr rate at high count rates.

Two enhancements to this electronic scheme will be considered. The double-ended coincidence time could be reduced below 5 ns to only consider detections occuring in the center of the fiber mat (flat portion not the bundles). This could reduce relative gamma-ray efficiency without sacrificing beta-particle efficiency. The double-ended 1-PE coincidence requirement for the first layer can be relaxed to a single-ended 1-PE detection when in coincidence with another layer. This could increase the efficiency for detecting the ^{85}Kr beta as a coincidence between the first two layers when the first layer uses 0.5-mm fibers.

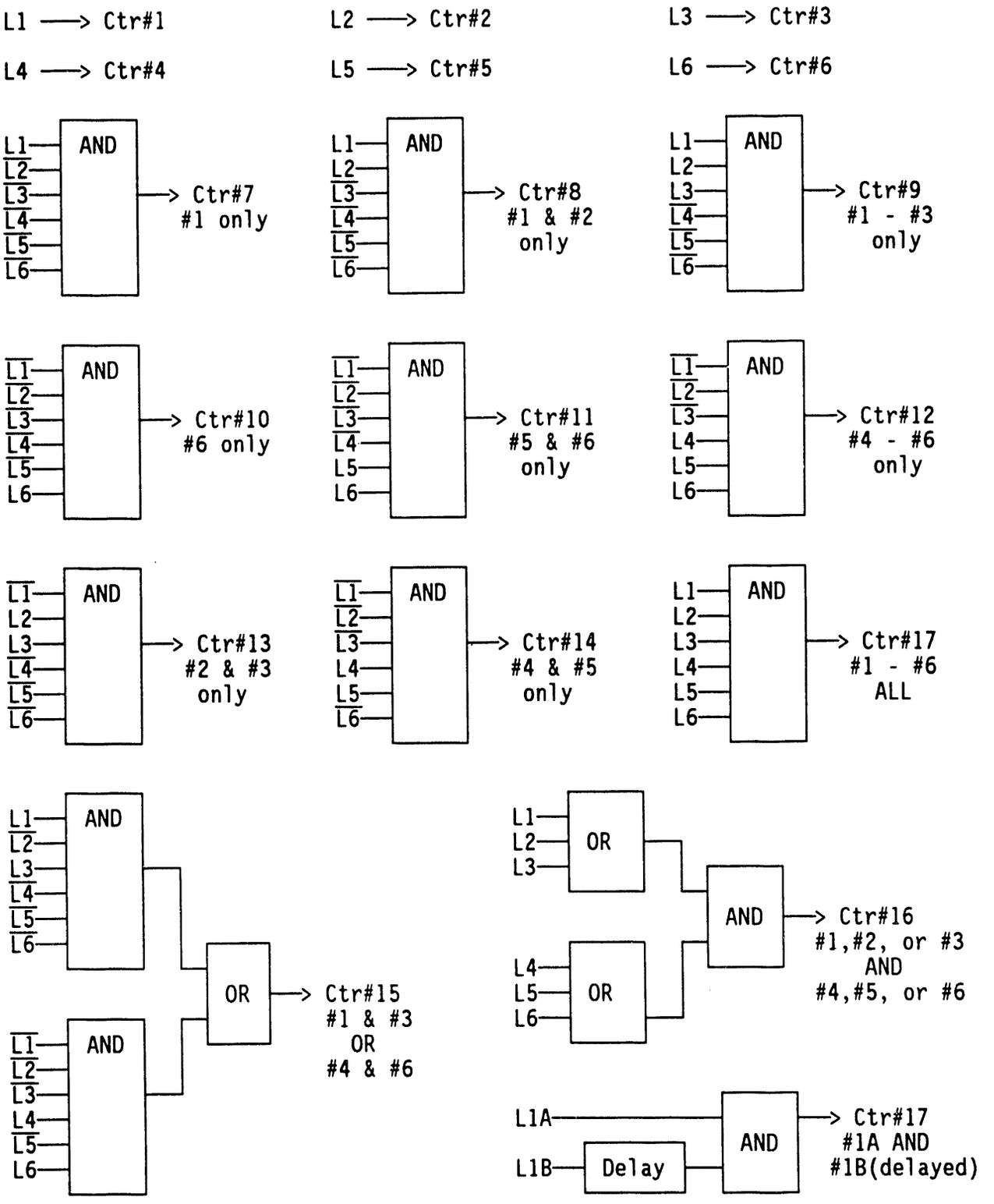

FIGURE 6. Intralayer Coincidence Logic for 6-Layer Segment

PROPOSED DEMONSTRATIONS

The laboratory demonstration sensor will utilize 15-cm-wide fiber optical ribbons and 3/4-inch-diameter PMTs. This laboratory sensor will be placed in a pipe section to which pure krypton gas can be added to demonstrate the ability to count low levels of ^{85}Kr activity. This laboratory demonstration sensor will provide maximum coincidence rate information, which will be used to determine the best data and analysis to obtain the most sensitivity to ^{85}Kr and minimize false alarms due to other gases (such as radon). The response of the laboratory sensors to several standard point sources will be determined to demonstrate and optimize the ability of the sensor to reject non-^{85}Kr sources. The idea of the several sources is to demonstrate the spatial uniformity over the sensor air volume and the ability to separate sources based on beta-energy and/or gamma-ray response. Pure gamma-ray response can be easily demonstrated by using sealed sources where the beta will not escape. Table 3 lists possible isotopic sources.

The diameter of the final prototype sensor is a tradeoff between higher detection efficiency per fiber at large diameter (due to large volume of gas near the outer wall) and better spatial uniformity (due to less variation in the beta path length through the air). Poor spatial uniformity reduces the ability to discriminate against higher-energy or lower-energy beta particles from other radioisotopes.

A small ^{36}Cl source will be used as a convenient analog for ^{85}Kr for mapping spatial response. The energetic ^{90}Y (daughter of ^{90}Sr) beta and energetic ^{234m}Pa (daughter of ^{238}U) will be used to demonstrate rejection of energetic beta particles. Both of these radioisotopes may be present in an air sample containing dust particles. The low-energy ^{147}Pm beta will be used to demonstrate rejection of low-energy beta particles.

The common background isotopes (^{137}Cs, ^{40}K, and ^{60}Co) will be considered to demonstrate gamma-ray rejection. The arms control impact of the other isotopes will be considered and the response of the sensor to these isotopes will be determined if desired. Some of these other isotopes have reasonable half-lives as well as slightly lower or slightly higher average beta particle energies, which would demonstrate the ability of the sensor to perform as a crude beta energy spectrometer.

TABLE 3. Possible Demonstration Sources

Source	Halflife	Beta Information	Gamma Information
^{85}Kr	10.72 yr	<251> max 687.4 keV 99.6%	None
^{36}Cl	3.0E5 yr	<246> max 709.2 keV 98.1%	None
^{90}Sr	28.5 yr	<196> max 546.0 keV 100%	None
^{90}Y	64.1 hr	<934> max 2,284 keV 99+%	2186.187 (1.4E-6%)
^{234m}Pa	1.17 m	<819> max 2.207 keV 98.6%	1001.0(0.65%) & others
^{234}Pa	6.70 hr	<215> max	131(20%) & 926(23%) & others
^{147}Pm	2.62 yr	<62> max 225 keV 99.99%	121.3(.0028%) 197.4(3E-7%)
COMMON BACKGROUND PROBLEM ISOTOPES			
^{137}Cs	30.17 yr	<188> max 1171 514	661.66(85.21%)
^{40}K	1.3E9 yr	<455> max 1312 keV 89.3%	1460.832(89.3%)
^{60}Co	5.27 yr	<96>	1173(99.90%) 1332(99.98%)
OTHER ISOTOPES OF POSSIBLE INTEREST			
^{133}Ba	10.54 yr	none	356(62.2%) & others to 384
^{32}Si	104 yr	<69> max 225 keV 100%	none
^{32}P	14.28 d	<695> max 1,710 keV 100%	none
^{89}Sr	50.52 d	<583> max 1492 keV 100-%	909.15(.0095%)
^{123}Sn	129.2 d	<523> max 1.42	1088.63% (0.6%)
^{170}Tm	128.6 d	<315> max 968 keV	84.3(3.2%)
^{186m}Re	2E5 yr	none	IT
^{186}Re	3.77 d	<323> max 1071 933	137(8.5%)
^{204}Tl	3.78 yr	<238> max 763(97.4%)	none
^{14}C	5730 yr	<49.5> max 157	none
^{39}Ar	269 yr	<218> max 565	none
^{42}Ar	32.9 yr	<233> max 600	none
^{129}I	1.6E7 yr	<41.5> max 192	39.6 (7.5%)
^{135}Cs	2.3E6 yr	<56> max 205	none

The laboratory demonstration will attempt to minimize the background rates to allow estimation of a minimum detectable level of ^{85}Kr. The ultimate background reduction for a ground based would sensor would require active anticoincidence shielding and passive low-Z material shielding. The laboratory demonstration sensor will not take full advantage of these shielding techniques until the most efficient detection modes are experimentally determined.

PNL-9469
UC-713
UC-506

DISTRIBUTION

No. of
Copies

OFFSITE

12 DOE/Office of Scientific and
Technical Information

Robert Hartley
AFTAC
1030 S. Highway A1A
Patrick AFB, FL 32925-3002

Leslie Casey
U.S. Department of Energy
Forrestal Building NN-20
1000 Independence Avenue, S.W.
Washington, DC 20585

ONSITE

DOE Richland Operations Office

R.B. Goranson

9 Pacific Northwest Laboratory

M.A. Knopf
R.A. Warner
B.D. Geelhood
Publishing Coordination
Technical Report Files (5)

DATE

FILMED

8/9/94

END